

## Scientific Article

# A Multi-Institutional Experience of MR-Guided Liver Stereotactic Body Radiation Therapy



Stephen A. Rosenberg MD <sup>a,b</sup>, Lauren E. Henke MD <sup>c</sup>,  
Narek Shaverdian MD <sup>d</sup>, Kathryn Mittauer PhD <sup>a</sup>,  
Andrzej P. Wojcieszynski MD <sup>a,e</sup>, Craig R. Hullett MD, PhD <sup>a</sup>,  
Mitchell Kamrava MD <sup>d</sup>, James Lamb PhD <sup>d</sup>, Minsong Cao <sup>d</sup>,  
Olga L. Green PhD <sup>c</sup>, Rojano Kashani PhD <sup>f</sup>, Bhudatt Paliwal PhD <sup>a</sup>,  
John Bayouth PhD <sup>a</sup>, Paul M. Harari MD <sup>a</sup>, Jeffrey R. Olsen MD <sup>g</sup>,  
Percy Lee MD <sup>d</sup>, Parag J. Parikh MD <sup>c</sup>, Michael Bassetti MD, PhD <sup>a,\*</sup>

<sup>a</sup>Department of Human Oncology, University of Wisconsin School of Medicine and Public Health, Madison, Wisconsin; <sup>b</sup>Department of Radiation Oncology, H. Lee Moffitt Cancer Center and Research Institute, Tampa, Florida; <sup>c</sup>Department of Radiation Oncology, Washington University School of Medicine, St. Louis, Missouri; <sup>d</sup>Department of Radiation Oncology, University of Los Angeles School of Medicine, Los Angeles, California; <sup>e</sup>Department of Radiation Oncology, Perelman School of Medicine, University of Pennsylvania, Philadelphia, Pennsylvania; <sup>f</sup>Department of Radiation Oncology, University of Michigan, Ann Arbor, Michigan; and <sup>g</sup>Department of Radiation Oncology, University of Colorado School of Medicine, Denver, Colorado

Received 1 June 2017; revised 5 August 2018; accepted 7 August 2018

## Abstract

**Purpose:** Daily magnetic resonance (MR)–guided radiation has the potential to improve stereotactic body radiation therapy (SBRT) for tumors of the liver. Magnetic resonance imaging (MRI) introduces unique variables that are untested clinically: electron return effect, MRI geometric distortion, MRI to radiation therapy isocenter uncertainty, multileaf collimator position error, and uncertainties with voxel size and tracking. All could lead to increased toxicity and/or local recurrences with SBRT. In this multi-institutional study, we hypothesized that direct visualization provided by MR guidance could allow the use of small treatment volumes to spare normal tissues while maintaining clinical outcomes despite the aforementioned uncertainties in MR-guided treatment.

**Methods and materials:** Patients with primary liver tumors or metastatic lesions treated with MR-guided liver SBRT were reviewed at 3 institutions. Toxicity was assessed using National Cancer

This work was presented as an oral presentation at ASTRO 2015, San Antonio, Texas.

Sources of support: This work had no specific funding.

Conflicts of interest: The authors have no conflicts of interest to disclose.

\* Corresponding author. 600 Highland Ave., Madison, WI 53792.

E-mail address: [bassetti@humonc.wisc.edu](mailto:bassetti@humonc.wisc.edu) (M. Bassetti).

<https://doi.org/10.1016/j.adro.2018.08.005>

2452-1094/© 2018 The Authors. Published by Elsevier Inc. on behalf of American Society for Radiation Oncology. This is an open access article under the CC BY-NC-ND license (<http://creativecommons.org/licenses/by-nc-nd/4.0/>).

Institute Common Terminology Criteria for Adverse Events Version 4. Freedom from local progression (FFLP) and overall survival were analyzed with the Kaplan-Meier method and  $\chi^2$  test.

**Results:** The study population consisted of 26 patients: 6 hepatocellular carcinomas, 2 cholangiocarcinomas, and 18 metastatic liver lesions (44% colorectal metastasis). The median follow-up was 21.2 months. The median dose delivered was 50 Gy at 10 Gy/fraction. No grade 4 or greater gastrointestinal toxicities were observed after treatment. The 1-year and 2-year overall survival in this cohort is 69% and 60%, respectively. At the median follow-up, FFLP for this cohort was 80.4%. FFLP for patients with hepatocellular carcinomas, colorectal metastasis, and all other lesions were 100%, 75%, and 83%, respectively.

**Conclusions:** This study describes the first clinical outcomes of MR-guided liver SBRT. Treatment was well tolerated by patients with excellent local control. This study lays the foundation for future dose escalation and adaptive treatment for liver-based primary malignancies and/or metastatic disease.

© 2018 The Authors. Published by Elsevier Inc. on behalf of American Society for Radiation Oncology. This is an open access article under the CC BY-NC-ND license (<http://creativecommons.org/licenses/by-nc-nd/4.0/>).

## Introduction

Improved local and systemic treatments have led to patients living longer in the setting of oligometastatic disease.<sup>1,2</sup> Ultimately, 50% of patients with solid tumor malignancies develop liver metastases.<sup>3</sup> In addition to metastatic disease, the rate of primary liver malignancies has tripled in the United States since the 1980s. There are more than 39,000 primary liver malignancies in the United States each year, with more than 27,000 deaths.<sup>4</sup> Local control of tumors within the liver is of pivotal importance for improving outcomes for patients with cancer.<sup>5,6</sup>

There are a multitude of treatment options for primary or secondary liver malignancies. Primary resection leads to excellent local control and is the preferred treatment modality. Only a small minority (<20%) of patients with liver lesions have tumors amenable to primary resection.<sup>7–10</sup> Other treatment modalities such as radiofrequency ablation (RFA) and transarterial chemoembolization (TACE) are often limited by location (ie, blood vessels, biliary tract, or liver dome) or tumor size. RFA and TACE are invasive procedures and may be associated with complications such as bleeding, infection, or liver decompensation.<sup>11,12</sup>

Stereotactic body radiation therapy (SBRT) is a relatively newer treatment modality for both primary and metastatic liver lesions that delivers ablative radiation doses to tumors. Single-institutional series of liver SBRT have reported local control rates from 50% to 90% depending on histologic type and tumor size.<sup>13–25</sup> Clinicians are often restricted in the use of liver SBRT secondary to dose limitations of the uninvolved liver and nearby normal organs (eg, kidney and bowel). To appropriately limit normal tissue dose and account for organ motion, multiple approaches have been developed, including abdominal compression, fiducial marker

placement, and spirometric breathing control.<sup>26,27</sup> Even with surrogates of motion (ie, fiducial placement), many liver tumors are not well visualized with x-ray imaging.

Magnetic resonance (MR)–guided treatment systems allow real-time visualization and tracking of the tumor itself, without using surrogate fiducial markers, and the normal tissues during SBRT. The benefits of MR-guided treatment include improved soft tissue visualization and tumor delineation. However, this technology is new, and clinical outcomes with this technology are unproven. Numerous obstacles must still be taken into account with MR-guided radiation treatment planning: electron return effect, MR imaging (MRI) geometric distortion, MRI to radiation therapy (RT) isocenter uncertainty, multileaf collimator (MLC) position error, and uncertainties with voxel size and tracking. All could lead to toxicity and/or local recurrences, particularly in the setting of small margins.

In this multi-institutional study, we hypothesized that direct visualization provided by MR guidance could allow small treatment volumes to spare normal tissue while maintaining clinical outcomes despite the aforementioned uncertainties in MR-guided targeting. If clinical outcomes are appropriate, this technology could then better be used for dose escalation and potentially adaptive treatment.

## Methods and materials

### Eligible patients

As part of an institutional review board–approved study, we reviewed patients between 2014 and 2017 at 3 institutions where they underwent MR-guided liver SBRT with the MRIdian System (ViewRay Inc., Mountain View, CA). Patients included had primary hepatocellular carcinoma (HCC) of the liver or metastatic tumors to the

liver for which surgery was not deemed an appropriate option. Patients had either Child-Pugh A or early B and 1 to 3 liver lesions. No strict cutoff on lesion size was placed on this population. Patients were not excluded if they had previous local or regional therapy for their liver lesion (ie, RFA, TACE).

## Simulation

Real-time MR-guided SBRT delivery has been previously described.<sup>28</sup> Briefly, patients underwent 0.35 T MRI on the MRIdian system. The treatment unit is an open, split solenoid 0.35 T MRI scanner combined with 3 co-planar cobalt sources. Treatment is delivered via intensity modulated RT. Patients underwent simulation using a thorax board or Vac-Lok bag immobilization. MRI coils were placed on the abdomen and directly under the patient or outside an immobilization device. No external respiratory motion management systems were employed (ie, abdominal compression, spirometry, or fiducial placement). True fast imaging (TRUFI) with steady state free precession images were obtained (3.33 ms TR (repetition time), 1.43 ms TE (echo time), 60° flip angle, 3 mm slice thickness, 40 × 40 × 43 cm field of view). This resulted in T2-/T1-weighted images. Tumor motion was evaluated with a real-time sagittal TRUFI cine MRI sequence (2.1 ms TR, 0.91 ms TE, 60° flip angle, 7 mm slice thickness, 4 frames per second). The patient's breath hold reproducibility and tolerance was evaluated at simulation. Patients underwent simulation with a free-breathing scan to assess motion. Organ and tumor motion was also assessed with a maximum inspiratory breath hold and/or a shallow breathing technique. If patients were unable to tolerate the simulation and cine because of claustrophobia or inadequate breath hold, they did not move forward with MR-based treatment.

Some patients who had metastatic lesions received gadoteric acid 20 minutes before simulation and each treatment as previously described.<sup>28</sup> On the same day as MRI simulation, patients underwent a computed tomography (CT) scan (free-breathing, 4-dimensional CT, depending on institution preference) in the treatment position. This was obtained for electron density data for dose calculations and aiding in outlining organs at risk (OARs) and tumor. Two institutions performed gating with maximum inspiratory breath hold for each patient treated (N = 16), and one institution used a modified shallow internal target volume or exhale-based setup for treatment (N = 10). The basis of this choice was each institution's different approach to patient reproducibility and comfort.

If tumor visualization was appropriate on simulation, the tracking for treatment was performed on the lesion. However, for some lesions, real-time sagittal TRUFI cine MRI provided inadequate tracking to deliver treatment. In

this context, tracking was done using a surrogate anatomy: portal vein, liver lobe, and so on. Tracking was only performed in 1 plane (sagittal) as standard practice at each institution.

## Treatment planning

A rigid registration of the 0.35 T simulation MRI scan and the CT simulation was created for treatment planning. The MRI was used as primary reference for contouring for 2 institutions and the CT for 1 institution. However, all available diagnostic information (TRUFI sequence, CT scan, and diagnostic MRI if available) was used for the contouring process. The gross tumor volume (GTV) was delineated; no clinical target volume expansion was made (GTV = clinical target volume). A 2- to 5-mm isotropic expansion was made to the planning target volume (PTV). The margin was chosen based multiple factors: cobalt source isocenter runout, MRI geometric distortion, uncertainty of position of the 3 cobalt head isocenter, MRI to RT isocenter, MLC position error, and uncertainties with voxel size and tracking. These variables are independent, and the sum of the square of these various uncertainties leads to a 2-mm margin. Additional margin was added (up to 3 mm) at the discretion of the treating physician. The final margin was individualized for each patient, taking into account each patient's individual factors, and was not decided a priori.

The MRI and CT planning scans were imported into the treatment planning system (ViewRay Inc). A Monte Carlo treatment planning algorithm (ViewRay Inc) was used with magnetic field corrections to account for the electron return effect. The treatment was prescribed to the PTV volume. Treatment plans had 12 to 15 beams per plan. Treatment planning goals varied across institutions but included mean liver dose <13 to 15 Gy, >700 cm<sup>3</sup> of liver less than 15 Gy (liver-GTV), and stomach and bowel V32-33 <0.5 cm<sup>3</sup> (Table E1; available online at <https://doi.org/10.1016/j.adro.2018.08.005>). These goals were not strict cutoffs, and final dosimetry balanced goals of care versus toxicity. Typically, patients were treated with 50 Gy in 5 fractions, but this varied depending on OAR and liver function. Typically we prescribed for at least 95% coverage of the prescribed dose unless restricted by OARs. However, this was heterogeneous across patients and institutions. To be considered SBRT and included in analysis, treatment must have been ≥30 Gy in total and ≥6 Gy/fraction. MR-guided RT plans have previously been found to be similar to conventional linear accelerator plans.<sup>29,30</sup>

## Treatment delivery

At the time of treatment, patients underwent an MRI scan for target and OAR alignment to the simulation. If

gadoxetic acid contrast was used to enhance tumor visualization at simulation, contrast was also given before each treatment.

A boundary region was used if maximum inspiratory breath hold was used for gating to ensure tumor was within the proper position. This boundary was less than or equal to the PTV. A sagittal TRUFI cine MRI sequence (2.1 ms TR, 0.91 ms TE, 60° flip angle, 7 mm slice thickness 35 × 35 field of view, 4 frames per a second) was acquired for patients undergoing treatment. This allows for tumor or tracking visualization during RT delivery via deformation/autosegmentation. A threshold of 90% to 95% of the GTV being within the boundary region was required for beam on. Patients were coached with audio feedback to optimize tumor time within the boundary structure. Daily adaptive treatment was not yet commonly employed across institutions at the time of this study.

The time in the treatment room was typically 40 to 60 minutes with 20 to 30 minutes of beam-on time. This significantly varied by dose rate of the cobalt sources across institutions and breathing reproducibility for each patient.

## Follow-up

Patients were seen in follow-up every 3 to 6 months. A typical follow-up included an interval history, physical examination, appropriate imaging (MRI abdomen, positron emission tomography/CT, or CT of the abdomen/pelvis), and laboratory values (eg, tumor makers and liver enzymes). Freedom from local progression (FFLP) was determined as a lack of an in-field or marginal failure at first progression.<sup>13,31</sup> FFLP and overall survival (OS) were analyzed with Kaplan-Meier and a  $\chi^2$  test. Toxicity was determined using National Cancer Institute Common Terminology Criteria for Adverse Events Version 4 as a chart review with a focus on grade 3 or higher toxicity. All patients were assessed for toxicity, FFLP, and OS. Secondary analysis of progression-free survival (PFS; progression locally, regionally, or distally) was also reported.

## Results

A description of the patient population treated at all institutions is shown in Table 1. A total of 26 patients who were treated with MR-guided liver SBRT were available for analysis. The majority of patients were male (65%). The average age at the time of treatment was 70 years (range, 30-90 years). Twenty patients (77%) had Child-Pugh A before treatment. The Child-Pugh status was unknown for 6 patients before SBRT. A variety of lesions were treated, including both metastatic and primary liver tumors: 8 colorectal adenocarcinoma, 6 HCC,

**Table 1** Summary of population treated with real-time MR-guided liver SBRT

Characteristic	n (%)
Age, median (range), y	70 (30-90)
Sex	
Male	17 (65%)
Female	9 (35%)
Histologic diagnosis	
Colorectal	8 (31%)
Hepatocellular carcinoma	6 (23%)
Lung	3 (12%)
Cholangiocarcinoma	2 (8%)
Pancreatic	1 (4%)
Sarcoma	1 (4%)
Head and neck	1 (4%)
Other	4 (15%)
Pretreatment Child-Pugh class	
A	20 (76.9%)
B	0 (0%)
C	0 (0%)
NA	6 (23.1%)
PTV (cm <sup>3</sup> ), median (range)	98.2 (13-2034)
Dose (Gy) to PTV, median (range)	50 (30-60)
Dose (Gy) per fraction, median (range)	10 (6-12)
Liver dose (Gy), median (range)	12.7 (3.2-21.9)
Posttreatment Child-Pugh class	
A	13 (50%)
B	1 (4%)
C	1 (4%)
NA	11 (42%)
GI toxicity	
Grade 3	2 (7.69%)
Grade 4-5	0 (0%)

Abbreviations: GI = gastrointestinal; MR = magnetic resonance; NA = not applicable; PTV = planning target volume; SBRT = stereotactic body radiation therapy.

Median follow-up is 21.2 months. Liver mean excludes dose from the gross tumor volume.

3 lung, 2 cholangiocarcinomas, 1 pancreas, 1 sarcoma, 1 head and neck, and 4 others. Given the variety of primary and metastatic tumors, there was a wide array of local and systemic pretreatment in this population. The median PTV size was 98.2 cm<sup>3</sup> (range, 13-2024). The majority of patients were treated with 50 Gy (range, 30-60 Gy) in 5 fractions (6-12 Gy/fraction). Treatments typically had a duty cycle (beam on time) of 80% to 85%. An example of a typical treatment plan and dose distribution is shown in Figure 1.

Treatment of this patient population was well tolerated. There was minimal grade 3 gastrointestinal (GI) toxicity (7.7%) (N = 2) at a median follow-up of 21.2 months. One patient developed a significant hilar stricture requiring a procedure. This patient had a large PTV size (>250 cm<sup>3</sup>) and mean liver dose of 21.9 Gy (liver-GTV). Another patient developed portal hypertension. Fifteen patients had pre- and posttreatment Child-Pugh

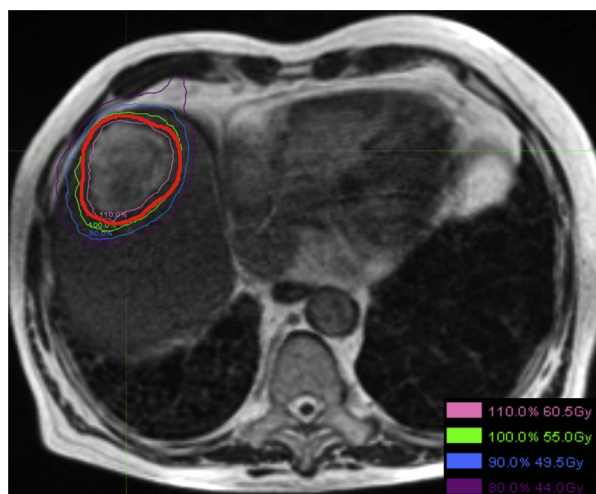


**Figure 1** Patient with liver metastasis with images showing simulation on the MRIdian system with the true fast imaging sequence and the dose distribution.

available for analysis (Table E2; available online at <https://doi.org/10.1016/j.adro.2018.08.005>). Two patients had a drop in Child-Pugh score in this population. A patient with a renal cell carcinoma treated to 40 Gy in 5 fractions had a drop in Child-Pugh score from A to B. This patient had a large-volume tumor (>900 cm<sup>3</sup>) that led to a higher than average liver mean dose of 18.9 Gy (liver-GTV). The second patient with a drop in Child-Pugh from A to C had an HCC with 4 prior TACE procedures. This patient was treated 50 Gy in 10 fractions and also had a high mean liver dose (20 Gy) (liver-GTV). This was the same patient who developed portal hypertension. No grade 4 or 5 toxicity was observed in this cohort. There was minimal to no skin toxicity in this group despite the use of a cobalt-based system.

FFLP and OS were analyzed for this group. At the median follow-up (21.2 months), the FFLP was 80.4% (Fig 2A). The 1-year and 2-year OS in this cohort was 69% and 60%, respectively (Fig 2B). Two patients had very short follow-up (approximately 2 months) with 1 patient dying 2 months after liver SBRT secondary to rapid distant progressive disease. There is no indication that patient died from radiation-related toxicity. The other patient was lost to follow-up.

FFLP varied based on tumor histology (Fig 3). The FFLP rates for patients with HCC were 100%. Patients with colorectal metastasis had a 75% FFLP. For all other primary or metastatic tumors combined, the FFLP was 83%. There were 2 local failures (transitional cell carcinoma of the renal pelvis and a renal cell carcinoma) among these 12 patients. Colorectal versus noncolorectal tumor histology had a higher frequency of local progression after SBRT with a trend toward significance ( $\chi^2$  [N = 26],  $P = .36$ ). The PFS (local, regional, or distant progression) in the entire cohort was 35% (9 patients

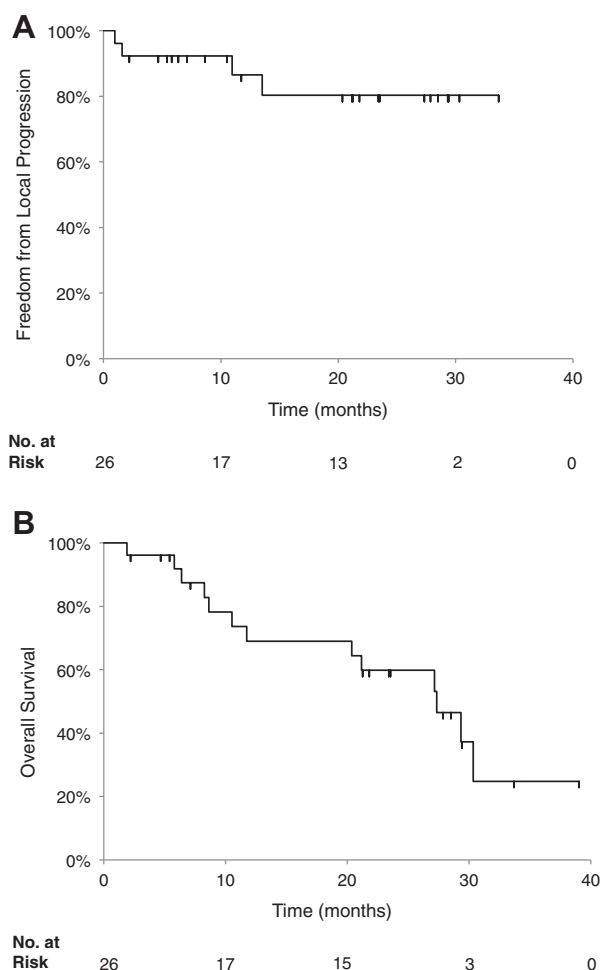


**Figure 2** Analysis of (A) freedom from local progression (FFLP) and (B) overall survival. Twenty-six patients were available for analysis. FFLP and OS were analyzed for this group. At the median follow-up (21.2 months), the FFLP was 80.4% (A). The 1-year and 2-year OS in this cohort was 69% and 60%, respectively (B).

without known progressive disease). The PFS for HCC, colorectal lesions, and other histologic tumor types was 33%, 25%, and 42%, respectively.

## Discussion

Treatment for liver SBRT is technically challenging, involving high doses, steep gradients, small margins, and moving tumors. MR guidance holds promise to ensure treatment accuracy through improved setup and direct visualization of treatment targets. As with any new technology, new sources of error and uncertainties exist. Notable uncertainties for MR-guided SBRT include electron return effect, MRI geometric distortion, MRI to RT isocenter uncertainty, MLC position error, and uncertainties with voxel size and tracking. It is important to

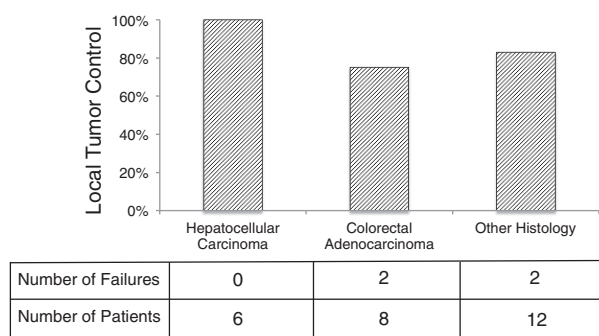


**Figure 3** Freedom from local progression (FFLP) varied by histologic diagnosis. Patients with hepatocellular carcinoma had a 100% FFLP. Patients with colorectal metastasis and all other histologic diagnoses had an FFLP of 75% and 83%, respectively. The FFLP was determined as of the most recent follow-up for each patient within this cohort. Colorectal metastasis trended toward decreased local control compared with other histologic tumor types ( $\chi^2$  [N = 26],  $P = .36$ ).

evaluate these clinically because they could lead to increased local recurrences and/or toxicity with SBRT.

This study is the first to describe the clinical outcomes of liver SBRT with real-time MR guidance. In this cohort the FFLP and OS of primary and metastatic liver tumors treated with MR-guided treatment are consistent with those previously reported in the literature (FFLP 80.4% and 2-year OS 60%). This includes the slightly lower local control rate of patients with colorectal metastasis (75%) compared with primary liver tumors or other metastatic lesions.<sup>13–19,21,24,25</sup> These results provide strong clinical evidence that MR-guided treatment is accurate in delivery in the clinical context of liver SBRT.

Minimal toxicity was identified in this treatment cohort. There were a small number of grade 3 GI toxicities (7.7%). No grade 4 or grade 5 toxicity was found with MR-guided treatment. Only 2 patients experienced a drop in Child-Pugh category. Most patients with grade 3 GI toxicity or a drop in Child-Pugh had previous multiple local therapies and/or high liver mean doses with treatment. This experience is in contrast to other reports of liver SBRT that sometimes indicate a drop in Child-Pugh in 20% to 30% of patients in addition to rates of 1% to 10% for grade 4 or 5 toxicity.<sup>32,33</sup>

As expected, despite cobalt sources, SBRT planned with multiple beam angles produced no significant skin reactions in this treatment population. Patients in the present study tolerated treatment extremely well, including a patient aged 90 years. These results are consistent with the literature reporting that SBRT is well tolerated with minimal adverse impact on quality of life.<sup>34</sup> The majority of radiation-induced liver disease occurs within the first 2 to 9 months after treatment.<sup>35,36</sup> Given our median follow-up of 21 months, we were likely able to capture the majority of any toxicity from MR-guided treatment.

The low toxicity found in this study is likely related to several factors, including the use of small treatment volumes and the ability to visualize tumors, liver, and other OARs during treatment (MRI cine). Visualization helps ensure greater accuracy and reproducibility in delivering the prescribed dose to the target. This also allows the use of small PTV margins that may be individualized based on patient characteristics (ie, reproducible breath hold) and characteristics of the physical aspects of the machine (eg, MRI geometric distortion, target tracking, MLC position error).

The cine MRI allows for tumor tracking in a single sagittal plane during treatment. Importantly, previous research has found that the majority of liver tumor motion is in the superoinferior and anteroposterior directions.<sup>37</sup> Therefore we are able to visualize the majority of tumor motion or surrogate anatomy during treatment. However, this leaves the possibility of unexpected tumor or patient motion in the medial/lateral dimension going unrecognized. The co-planar orientation of the beams results in the least gradient in the axial plane, which helps address uncertainty. The inherent penumbra of cobalt in this MRIdian system also helps address uncertainty that accompanies tumor tracking. However, this feature also limits the conformality of our treatment plans compared with a linear accelerator (linac)–based approach. Small margins help compensate for the penumbra of the cobalt-based compared with traditional approaches with larger PTV expansions. Linac-based MR-guided RT is now clinically available. Balancing tightly conformal treatment, MR-guided linac-based approaches and PTV margin size will be important moving forward.

The small sample size, short follow-up, retrospective analysis, and heterogeneous group of patients are known limitations of this analysis. However, the study aimed to determine if we could overcome the unique obstacles of MR-guided treatment to deliver accurate and well-tolerated radiation in the technically challenging setting of liver SBRT. This study helps establish that MR-guided treatment is well tolerated and effective in the clinic despite these obstacles. Although MR-guided treatment may be limited to certain facilities, it is important to note that this technology is increasing across the United States and abroad. With the dissemination of this technology, safely and appropriately delivering liver SBRT will be imperative.

Despite the success of MR-guided treatment for most patients, local failures were noted in our treatment cohort. A review of patients with local progression does reveal that normal organs at risk (eg, bowel, kidney) may be a limiting factor in delivering ablative radiation doses to liver tumors. An example of such a failure is a patient with a colorectal metastatic lesion in the medial lobe of the liver. Figure 4 shows the coronal view of the TRUFI sequence of the patient's MR-guided radiation plan. The nearby bowel limited dose to the inferior aspect of the

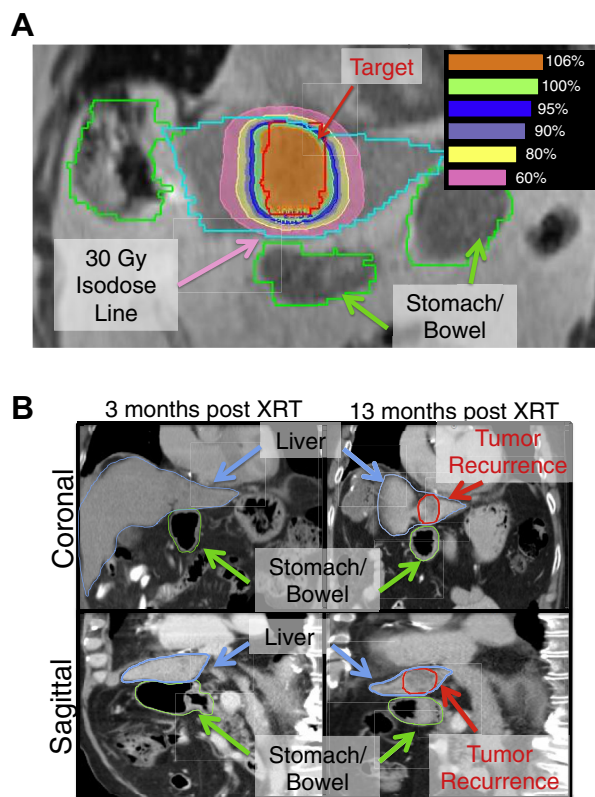


**Figure 4** (A) Coronal true fast imaging (TRUFI) sequence of a magnetic resonance (MR)-guided radiation therapy plan for a patient with colorectal liver metastasis. There is a close relationship with the bilobed lesion (planning target volume, red) in the medial liver in approximation to the bowel and the heart. The patient underwent MR-guided radiation therapy delivering 50 Gy in 5 fractions. The patient's follow-up scans at 3 and 13 months (B) show initial response followed by local progression. Progression of this patient's tumor is likely secondary to inadequate dosing of the tumor because of nearby organs at risk. This patient may have benefited from daily adaptive treatment to decrease dose to bowel or heart while maintaining ablative doses to the tumor. (A color version of this figure is available at <https://doi.org/10.1016/j.adro.2018.08.005>.)

tumor, and the heart limited dose to the superior aspect of the tumor. This may have contributed to the development of a local failure for this patient (Fig 4B). Studies of dose escalation indicate improved local control at higher doses of liver SBRT.<sup>38</sup> However, dose escalation to tumors may be limited secondary to nearby organs at risk. Adaptive MR-guided RT was not yet standard in our clinics when this patient was treated. If this had been available, this patient may have benefited from such an approach.

Per our review of patients, there remains significant interfractional motion of these organs as risk, as well as heterogeneity across patients (unpublished). With real-time visualization, we can potentially adapt treatment daily and potentially better personalize RT doses. Particularly for tumors near the liver edge, direct visualization during treatment allows confidence to treat with

high doses near organs such as bowel or stomach, where position uncertainty could lead to a dose that exceeds their tolerance. This may be of particular importance for tumors with slightly lower local control rates. For example, the FFLP for this population with colorectal metastasis was 75%, these patients may benefit from further dose escalation.<sup>38</sup> These colorectal patients also stand to gain the most because in some patients truly ablative control may offer the possibility of curative treatment similar to surgical resection.

The ability to adapt treatment to these tumor or anatomic changes on a daily basis with direct MRI visualization provides confidence in the dose to OARs, suggesting the feasibility of further dose-escalation studies. The ability to adapt treatment daily on the MRIdian system based on functional MRI sequences is currently in development and may also work to improve outcomes. This requires a detailed quality assurance process and recontouring OARs and targets each day.<sup>39,40</sup> Real-time MR guidance and daily plan adaptation provides the opportunity for further dose escalation that can be systemically explored in controlled clinical trials that are currently in development in our institutions. This multi-institutional study of a first experience with MR-guided liver SBRT will lay the foundation for further prospective studies.

## Conclusion

MR-guided liver SBRT provides local control rates consistent with those in the literature for metastatic and primary lesions with minimal toxicity. This suggests currently available MR-guided treatments account well for new sources of uncertainty associated with MR-guided treatment in a challenging clinical context. MR guidance allows the delivery of liver SBRT without the use of indirect or invasive means of respiratory motion management such as fiducial placement, spirometric breathing control, or abdominal compression. The limited toxicity reported to date with real-time MR-guided liver SBRT opens the opportunity to investigate plan adaptation and dose escalation to further improve outcomes for patients with tumors near critical organs.

## Supplementary data

Supplementary material for this article (<https://doi.org/10.1016/j.adro.2018.08.005>) can be found at [www.advancesradonc.org](http://www.advancesradonc.org).

## References

1. Weichselbaum RR, Hellman S. Oligometastases revisited. *Nat Rev Clin Oncol*. 2011;8:378-382.

2. Alongi F, Arcangeli S, Filippi AR, Ricardi U, Scorsetti M. Review and uses of stereotactic body radiation therapy for oligometastases. *Oncologist*. 2012;17:1100-1107.
3. Ananthakrishnan A, Gogineni V, Saeian K. Epidemiology of primary and secondary liver cancers. *Semin Intervent Radiol*. 2006;23:47-63.
4. American Cancer Society. *Cancer Facts & Figures 2017*. Atlanta: American Cancer Society; 2017.
5. Bengmark S, Hafström L. The natural history of primary and secondary malignant tumors of the liver. II. The prognosis for patients with hepatic metastases from gastric carcinoma verified by laparotomy and postmortem examination. *Digestion*. 1969;2:179-186.
6. Tomlinson JS, Jarnagin WR, DeMatteo RP, et al. Actual 10-year survival after resection of colorectal liver metastases defines cure. *J Clin Oncol*. 2007;25:4575-4580.
7. Wei AC, Greig PD, Grant D, Taylor B, Langer B, Gallinger S. Survival after hepatic resection for colorectal metastases: a 10-year experience. *Ann Surg Oncol*. 2006;13:668-676.
8. Fong Y, Fortner J, Sun RL, Brennan MF, Blumgart LH. Clinical score for predicting recurrence after hepatic resection for metastatic colorectal cancer: Analysis of 1001 consecutive cases. *Ann Surg*. 1999;230:309-318. discussion 318-321.
9. Agrawal S, Belghiti J. Oncologic resection for malignant tumors of the liver. *Ann Surg*. 2011;253:656-665.
10. Smith JJ, D'Angelica MI. Surgical management of hepatic metastases of colorectal cancer. *Hematol Oncol Clin North Am*. 2015;29:61-84.
11. Wong SL, Mangu PB, Choti MA, et al. American Society of Clinical Oncology 2009 clinical evidence review on radiofrequency ablation of hepatic metastases from colorectal cancer. *J Clin Oncol*. 2010;28:493-508.
12. Burrell M, Reig M, Forner A, et al. Survival of patients with hepatocellular carcinoma treated by transarterial chemoembolisation (TACE) using drug eluting beads. Implications for clinical practice and trial design. *J Hepatol*. 2012;56:1330-1335.
13. Liu E, Stenmark MH, Schipper MJ, et al. Stereotactic body radiation therapy for primary and metastatic liver tumors. *Transl Oncol*. 2013;6:442-446.
14. Herfarth KK, Debus J, Lohr F, et al. Stereotactic single-dose radiation therapy of liver tumors: Results of a phase I/II trial. *J Clin Oncol*. 2001;19:164-170.
15. Rusthoven KE, Kavanagh BD, Cardenas H, et al. Multi-institutional phase I/II trial of stereotactic body radiation therapy for liver metastases. *J Clin Oncol*. 2009;27:1572-1578.
16. Chang DT, Swaminath A, Kozak M, et al. Stereotactic body radiotherapy for colorectal liver metastases: A pooled analysis. *Cancer*. 2011;117:4060-4069.
17. Wulf J, Guckenberger M, Haedinger U, et al. Stereotactic radiotherapy of primary liver cancer and hepatic metastases. *Acta Oncol*. 2006;45:838-847.
18. Scorsetti M, Clerici E, Comito T. Stereotactic body radiation therapy for liver metastases. *J Gastrointest Oncol*. 2014;5:190-197.
19. Scorsetti M, Arcangeli S, Tozzi A, et al. Is stereotactic body radiation therapy an attractive option for unresectable liver metastases? A preliminary report from a phase 2 trial. *Int J Radiat Oncol Biol Phys*. 2013;86:336-342.
20. Bujold A, Massey CA, Kim JJ, et al. Sequential phase I and II trials of stereotactic body radiotherapy for locally advanced hepatocellular carcinoma. *J Clin Oncol*. 2013;31:1631-1639.
21. Hoyer M, Roed H, Traberg Hansen A, et al. Phase II study on stereotactic body radiotherapy of colorectal metastases. *Acta Oncol*. 2006;45:823-830.
22. Meyer JJ, Foster RD, Lev-Cohain N, et al. A phase I dose-escalation trial of single-fraction stereotactic radiation therapy for liver metastases. *Ann Surg Oncol*. 2016;23:218-224.
23. Méndez Romero A, Wunderink W, Hussain SM, et al. Stereotactic body radiation therapy for primary and metastatic liver tumors: A single institution phase I-II study. *Acta Oncol*. 2006;45:831-837.
24. Lee MT, Kim JJ, Dinniwell R, et al. Phase I study of individualized stereotactic body radiotherapy of liver metastases. *J Clin Oncol*. 2009;27:1585-1591.
25. Andolino DL, Johnson CS, Maluccio M, et al. Stereotactic body radiotherapy for primary hepatocellular carcinoma. *Int J Radiat Oncol Biol Phys*. 2011;81:e447-e453.
26. Dawson LA, Brock KK, Kazanjian S, et al. The reproducibility of organ position using active breathing control (ABC) during liver radiotherapy. *Int J Radiat Oncol Biol Phys*. 2001;51:1410-1421.
27. Eccles C, Brock KK, Bissonnette JP, Hawkins M, Dawson LA. Reproducibility of liver position using active breathing coordinator for liver cancer radiotherapy. *Int J Radiat Oncol Biol Phys*. 2006;64:751-759.
28. Wojcieszynski AP, Rosenberg SA, Brower JV, et al. Gadaxetate for direct tumor therapy and tracking with real-time MRI-guided stereotactic body radiation therapy of the liver. *Radiother Oncol*. 2016;118:416-418.
29. Wooten HO, Green O, Yang M, et al. Quality of intensity modulated radiation therapy treatment plans using a <sup>60</sup>Co Magnetic resonance image guidance radiation therapy system. *Int J Radiat Oncol Biol Phys*. 2015;92:771-778.
30. Kishan AU, Cao M, Wang PC, et al. Feasibility of magnetic resonance imaging-guided liver stereotactic body radiation therapy: A comparison between modulated tri-cobalt-60 teletherapy and linear accelerator-based intensity modulated radiation therapy. *Pract Radiat Oncol*. 2015;5:330-337.
31. Chan JL, Lee SW, Fraass BA, et al. Survival and failure patterns of high-grade gliomas after three-dimensional conformal radiotherapy. *J Clin Oncol*. 2002;20:1635-1642.
32. Dyk P, Weiner A, Badiyan S, Myerson R, Parikh P, Olsen J. Effect of high-dose stereotactic body radiation therapy on liver function in the treatment of primary and metastatic liver malignancies using the Child-Pugh score classification system. *Pract Radiat Oncol*. 2015;5:176-182.
33. Weiner AA, Olsen J, Ma D, et al. Stereotactic body radiotherapy for primary hepatic malignancies. Report of a phase I/II institutional study. *Radiother Oncol*. 2016;121:79-85.
34. Feng M, Brunner TB, Ben-Josef E. Stereotactic body radiation therapy for liver cancer: Effective therapy with minimal impact on quality of life. *Int J Radiat Oncol Biol Phys*. 2015;93:26-28.
35. Dawson LA, Normolle D, Balter JM, McGinn CJ, Lawrence TS, Ten Haken RK. Analysis of radiation-induced liver disease using the Lyman NTCP model. *Int J Radiat Oncol Biol Phys*. 2002;53:810-821.
36. Pan CC, Kavanagh BD, Dawson LA, et al. Radiation-associated liver injury. *Int J Radiat Oncol Biol Phys*. 2010;76(3 Suppl):S94-S100.
37. Case RB, Moseley DJ, Sonke JJ, et al. Interfraction and intrafraction changes in amplitude of breathing motion in stereotactic liver radiotherapy. *Int J Radiat Oncol Biol Phys*. 2010;77:918-925.
38. Rule W, Timmerman R, Tong L, et al. Phase I dose-escalation study of stereotactic body radiotherapy in patients with hepatic metastases. *Ann Surg Oncol*. 2011;18:1081-1087.
39. Henke L, Kashani R, Robinson C, et al. Phase I trial of stereotactic MR-guided online adaptive radiation therapy (SMART) for the treatment of oligometastatic or unresectable primary malignancies of the abdomen. *Radiother Oncol*. 2018;126:519-526.
40. Mittauer K, Paliwal B, Hill P, et al. A new era of image guidance with magnetic resonance-guided radiation therapy for abdominal and thoracic malignancies. *Cureus*. 2018;10:e2422.